

Cell Viability and Migration Study of Hydroxyapatite Encapsulated Silica Aerogel (Haesa) towards Normal Human Fibroblast Cells

Nor Suriani Sani^a, Nik Ahmad Nizam Nik Malek^{a*}, Khairunadwa Jemon^a, Mohammed Rafiq Abdul Kadir^b, Halimaton Hamdan^c

^a Faculty of Biosciences and Medical Engineering, Universiti Teknologi Malaysia, 81310 Skudai, Johor, Malaysia

^b Medical Devices and Technology Group (MEDITEG), Faculty of Biosciences and Medical Engineering, Universiti Teknologi Malaysia, 81310 Skudai, Johor, Malaysia

^c Razak School of Engineering & Advanced Technology, Universiti Teknologi Malaysia, 54100, Kuala Lumpur, Malaysia

* Corresponding author: niknizam@fbb.utm.my (N.A.N.N. Malek)

INTRODUCTION

Wound healing is essential for the restoration of the skin. During this process, cells at the wound edges proliferate and migrate, leading to re-epithelialization of the wound surface (Justus *et al.* 2013). The ability of the cells to migrate allows them to change their position within tissues or between different organs (Yue *et al.* 2010). However, one of the major challenges in maxillofacial surgeries is slow cell regeneration in chronic wounds that caused by pathological or traumatic conditions (Fu *et al.* 2011). This chronic wound is typically difficult to heal naturally (Mastrogiacomo *et al.* 2005) which can cause the damage of tissue if too long in inflammatory phase (Perumal *et al.* 2014). Although inflammation is a necessary part of the normal healing process but the presence of macrophage on wound bed can prevent the subsequent proliferative phase. Hence, tissue engineering has emerged with a focus to develop alternative biomaterial that can replace the conventional wound dressings such as bandages, cotton wool and gauzes which passively provide wound recovery (Bohner 2010, Dutta *et al.* 2015).

Hydroxyapatite (HA) has been widely developed during the past few decades due to its biocompatibility and excellent stability in human body (Hench 1991, Salinas and Vallet-Regí 2013). HA is a major mineral component in natural bone and because of that, it has an excellent biocompatibility (Orlovskii *et al.* 2002). Recently, HA has been used as a semi-permanent filler in non-surgical options for treating wrinkles and textural changes in skin rejuvenation (Buck *et al.* 2009, Kuhne and Imhof 2012). The best known brand of cosmetic fillers based on HA are Radiess, which consists of small HA microspheres (particles) suspended in a gel-like solution and KaliLight, the functionalized hydroxyapatite (Jacovella 2008, Srl 2017). The most common uses of HA-based cosmetic fillers are moderate-to-deep wrinkles, facial folds, loss of facial fat (lipoatrophy) and similar problems (Buck *et al.* 2009, Funt and Pavicic 2013). HA has a capability of providing an optimum environment around the wound and delivering active ingredients or directly interacting with cells in the local wound environment to facilitate wound healing (Kawai *et al.* 2011). It can induce the generation of new cells and support cell growth which leads to the decrease of fine line and deep wrinkles volume (Jacovella 2008). However, HA shows some drawbacks when compared with other bioactive materials. Although HA has high biocompatibility and bioactivity, it is inherently brittle and its resorbability are poor (Rahaman *et al.* 2011, Dutta *et al.* 2015). HA-based fillers actively degraded and have to be re-injected every year to maintain results beside, swelling at the injection site is relatively common (Buck *et al.* 2009). Thus, limit the clinical application of this material. Various methods such as refining the

microstructure of HA and incorporating reinforcing phases have been used to improve the biocompatibility of HA (Vallet-Regí and Arcos 2005, Thian *et al.* 2007, Bohner 2009).

The positive effect of the silica in the cell growth (Henstock *et al.* 2015) causing interests by the researchers to work on with silica-substituted HA as advanced bioactive ceramic (Bohner 2009). The incorporation of silica into HA has been shown to significantly increased the rate of bone apposition to HA bioceramic implants (Porter *et al.* 2003). Silica was reported to be important in enhancing the biocompatibility of HA (Rivera-Muñoz *et al.* 2011). It is due to the existent of silanol groups and resorption of silica during treatment and cells are positively influenced by this released phenomenon (Li *et al.* 1994, Takadama *et al.* 2001, Nayak *et al.* 2010). Since the formation of apatite layer depends on silanol groups on the silica surface, heat treated silica glass at 900°C that can reduce silanol groups on its surfaces distorts its resorbability characteristic (Ylänen *et al.* 2000). Hence, the sintering process involved in the synthesis of conventional silica glass can cause the reduction of silanol groups, thus lowering its bioactivity (Owens *et al.* 2016). Therefore, it is crucial to develop a new class of pure silica gel which its synthesis route and its properties are compatible with human body. SA is an emerging silica-based nanomaterial and due to its amorphous microstructure which consists of nano-sized pores created from linked particles (He *et al.* 2015), SA exhibits many desirable and unique properties in biomedical applications (Cai *et al.* 2014). Previous findings reported that the composite SA consists of crosslinked dialdehyde nanocellulose fibres and collagen, with a porosity of 93%, water absorption ratio of 3000% and good biocompatibility with fibroblast cells, making this material suitable for wound dressing applications (Lu *et al.* 2014). The good biocompatibility of SA as well as high level of cell activity and proliferation of human cells indicate that the SA has the potential to be used as a carrier vehicle for medical application (Lu *et al.* 2014).

In this work, HA was encapsulated into silica aerogel (SA) network via an aqueous sol-gel ambient-pressure drying (APD) technique. A newly modified aqueous route for the synthesis of HAESA using RHA as a cheap silicon precursor for the production of pure silicate solution was developed. The unique solubility behaviour of amorphous silica enables it to be extracted in pure form from RHA by simple dissolution technique under alkaline conditions (Listorini *et al.* 1996). Fabrication of HAESA, the unique combination of encapsulated HA and SA, will extensively elevate the biocompatibility and biofunctionality of fibroblast cells. Early study proved that the high release of calcium and phosphate from HA that could contribute to the alteration of the cell membrane and cell

apoptosis was delayed by covering the HA particles with fluorapatite network (Rodríguez-Lorenzo and Gross 2003). Therefore, the encapsulation route will offer better cell-material interface integrity of the HAESA (Wang *et al.* 2015). Thus, enabling the HAESA to be used as a carrier and cell delivery vehicle, with enhanced performance such as for wound care application (Lu *et al.* 2014).

MATERIALS AND METHOD

Synthesis of hydroxyapatite encapsulated silica aerogel

For the preparation of HAESA, HA powder (Sigma, 99%) at 0.5 wt.% ratio of HA/SiO₂ was immersed in an extracted sodium silicate (Na₂SiO₃) solution prepared from the RHA containing 10.24 wt.% of silica. The specific range of the HA/SiO₂ ratio that was used in this experiment was based on known characteristics of the hybrid sample obtained from literatures, such as their structural stability, toxicity level and also their availability (Hing *et al.* 2006, Thian *et al.* 2007, Shie *et al.* 2011). Then, the HAESA gel was prepared by acidifying the mixture with sufficient amount of concentrated H₂SO₄ (Merck, 97%) in a Teflon beaker. The aqueous gel was then aged at room temperature for 2 days to allow the formation of the silica framework. The wet gel was then washed with double-distilled water to remove excess impurities and the remaining sodium sulphate salt. Water in the gel was extracted by a solvent extraction technique, using acetone (Merck). Finally, the HAESA was dried by the APD technique at 40°C, which is close to the boiling point of acetone until a constant weight was obtained. The bulk sample density was measured from the dimensions of the sample. The dried powder of HAESA was then stored in an airtight Teflon bottle at room temperature. SA was also synthesized by the same method but without HA as a comparison with the HAESA. The bulk sample density was calculated as follows (Zhang and Ma 1999):

$$\text{Bulk sample density } (\rho) = \text{Mass of dried sample (g)} / \text{Volume of sample (cm}^3\text{)} \quad (1)$$

A leaching test was performed for the samples to confirm that all immersed HA were immobilized in the SA and the recorded cell bioactivity was due to the encapsulated HA, rather than other species in the reaction vessel (Sani *et al.* 2011). The leaching test was carried out by determining the presence of phosphate ions (mg/L) in the filtrate and extracted water obtained from the previously prepared gel using a phosphate analysis kit (NANOCOLOR; Standard Test 1-77; Macherey-Nagel, Germany).

Sample characterization

The SA, HAESA and HA were characterized by Fourier transform-infrared (FTIR) spectroscopy (Thermo Scientific Nicolet iS5 with OMNIC software) using the KBr method. Approximately, the sample was ground with KBr in a ratio of 1/100 (SA/KBr), using a mortar and pestle. The mixture was then pressed at 7 tonnes to form a KBr disk. The disk was put on the sample holder and the FTIR spectrum of the sample was recorded in the wavenumber range of 350 to 4000 cm⁻¹. The phase of each sample was identified using an X-ray diffraction (XRD) (Bruker; D8 advance, USA) instrument. XRD pattern was recorded with CuK_α radiation at λ = 1.5406 Å at 40 kV and 20 mA in the range of 2θ = 5° to 55°, with a scanning speed of 0.05° per second. The morphology, size, shape and arrangement of the particles in sample of the material was observed using field emission-scanning electron microscopy (FESEM) (JSM 6701F model, JEOL, USA) at an emission current of 2.00 kV, with a working distance of 3.0 mm and probe current of 8 kV. The elemental analysis of samples was determined using Energy Dispersive X-Ray (EDX) spectrometer (model EX-2300 BU, JEOL). The EDX analysis was carried out with the emission current of 15.0 kV with a working distance of 8.0 mm and probe current of 14 kV.

Cell viability assay

Cell viability of SA, HAESA and HA against HSF 1184 were quantified using an MTT [3-(4,5-dimethylthiazol-2-yl)-2,5-diphenyltetrazolium-bromide] assay (Invitrogen, Thermo Fisher Scientific, USA). MTT is cleaved in the mitochondria of all living cells that metabolically active and causes the colourless compound is known as tetrazolium, changing into a dark purple formazan crystal product (Freshney 2005). Proliferating cells which are more metabolically active than non-proliferating cells were actively cleaved MTT to a dark purple formazan crystal. Thus, the amount of formazan generated is directly proportional to the number of living cells in a cell population (Aminian *et al.* 2011). In this study, the MTT assay of SA, HAESA and HA were determined by directly contacted the 0.1 mm height, 13 mm diameter discs of the samples with HSF 1184 for 24 and 48 hours. Prior to the experiment, the samples were rinsed with 1× phosphate buffer saline (PBS) (Gibco) and then sterilized under UV lamp for 30 minutes, per each side of disc. Then, all samples were immersed in the complete DMEM solution for 15 minutes. The cells were seeded (1.0 × 10⁵ cells per well) in 24-well microtitre plates (1.0 ml per well), then incubated at 37°C in a 5% CO₂ atmosphere for 24 hours. After 24 hours of incubation, each of the sterilized samples was then placed directly on a confluent monolayer of cells and incubated for another period of time. After 24 and 48 additional hours of incubation, all media were removed from the well and were replaced with 700 μL of fresh complete DMEM. About 70 μL of 5 mg/mL MTT solution in PBS was added to each well. The plates were wrapped with aluminium foil as the MTT solution is light-sensitive. All plates were then incubated for 4 hours at 37°C. After incubation, 150 μL mixtures of the medium and MTT solution were removed from each well and 350 μL of DMSO was added into each well to dissolve the purple formazan crystal product. All samples were then removed from the cell cultures and the absorbance of formazan which was produced from the MTT was detected at λ_{540 nm} using a 96-well plate reader (ELISA Microplate Reader, Epoch, Biotek). The cell viability was calculated using the following formula (Rismanchian *et al.* 2013):

$$\text{Cell Viability (\%)} = \frac{\text{Mean OD of treated cells} - \text{Mean OD of blank}}{\text{Mean OD of untreated cells} - \text{Mean OD of blank}} \times 100 \quad (2)$$

Cell migration assay

The effect of the sample on the migration and healing ability of HSF 1184 was investigated by cell migration assay. This test was initiated by rinsing 0.1 mm height, 13 mm diameter disc of HAESA with 1× PBS and then, sterilized under UV lamp for 30 minutes per each side of a disc. Then, the sterilized sample was immersed in 1 mL of complete DMEM solution for 2, 5 and 7 days. The treated media was sterilized filter into 15 mL centrifuge tube and stored at 4°C. The cells were seeded (1.0 × 10⁶ cells per well) in 6-well microtitre plates (2.0 ml per well) and then, incubated at 37°C in a 5% CO₂ atmosphere and grown to confluence for 24 hours. After 24 hours of incubation, the confluent monolayer of cells was scratched with a 100 μL pipette tip to create an artificial wound gap. The cells were replenished with the treated media that contain extracted samples (HAESA-extract-2dys, HAESA-extract-5dys and HAESA-extract-7dys). The images of the plates were taken at the same location using an inverted optical microscope (Nikon Eclipse TS100) after 0, 6, 12 and 24 hours. The healing and migration behaviour of HSF 1184 were quantitatively evaluated using ImageJ 1.50i (National Institute of Health, Bethesda, MD, USA). The closure area was calculated using the following formula (Yue *et al.* 2010):

$$\text{Closure Area (\%)} = 1 - (\text{Scratch Area}_t / \text{Scratch Area}_0) \times 100 \quad (3)$$

Statistical analysis

All values represent the mean of three independent experiments. In each experiment, the data were collected in triplicate for each sample and were used to calculate the mean. All results are expressed as the mean \pm standard deviation (SD). The statistical analysis was performed using a two-way ANOVA with a Tukey post-hoc test, GraphPad Prism v.6.01 (GraphPad Software Inc., USA) at the 95% confidence level, with a p value < 0.05 considered to be of statistical significance.

RESULTS AND DISCUSSION

Physicochemical properties of hydroxyapatite encapsulated silica aerogel

The physicochemical properties of HAESA were determined using FTIR spectroscopy, XRD, FESEM and EDX. Fig. 1 show photographs, FTIR spectra and XRD patterns of SA, HAESA and free HA whereas Fig. 2 show FESEM micrographs and elemental analysis of major elements of these materials.

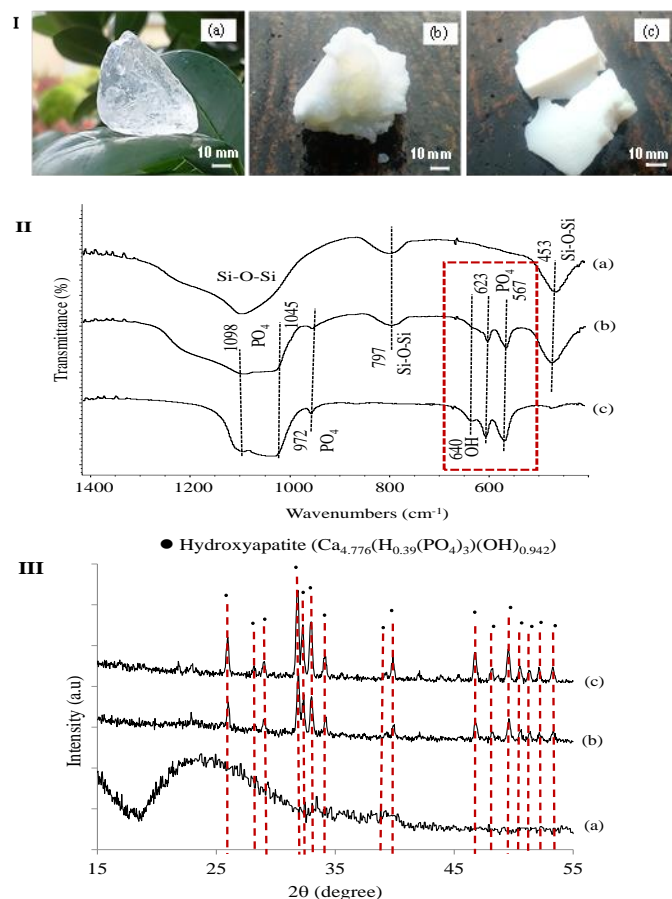


Fig. 1 (I) Photographs, (II) FTIR spectra and (III) XRD patterns of (a) SA, (b) HAESA and (c) free HA on spider plant.

From the observations on the physical appearance of each sample (Fig. 1 I), it was found that a semi-transparent and sky-blue solid SA with an average bulk density of $0.0809 \pm 0.0012 \text{ g/cm}^3$ was transformed into a dense and shiny opaque of irregular shaped HAESA with a bulk sample density of $0.0989 \pm 0.0014 \text{ g/cm}^3$ signified the existence of the smooth surface of white-coloured brittle encapsulated HA. The leaching test confirmed that almost all HA

particles were successfully immobilized in the SA networks of the synthesized HAESA. FTIR (Fig. 1 II) analyses confirm that all fingerprints of SA and HA peaks are preserved after the encapsulation process thus validates that HA existed in the HAESA and the structure of the encapsulated HA is well-maintained inside the SA networks. XRD (Fig. 1 III) analysis reveals HA particles were well-dispersed into SA as the crystalline structure of HA remained even after the encapsulation process. The structure of the HAESA was not converted to other phases and there were no impurities in the product after the encapsulation process.

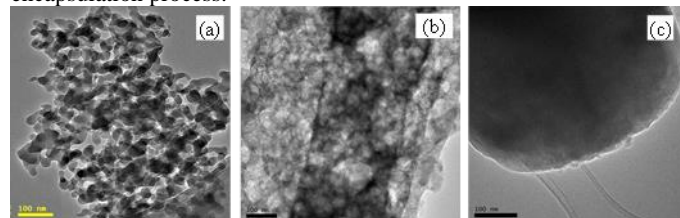


Fig. 2 TEM micrographs of (a) SA, (b) HAESA and (c) free HA.

TEM (Fig. 2) revealed that SA and HAESA were successfully synthesized in nano-sized particles in the range of 20 to 50 nm via the aqueous sol-gel ambient-pressure drying (APD) technique. The uniform and interconnected pores with homogeneous nano-spherical particles SA were changed to denser morphology and particle size are reduced after the encapsulation process. The morphological analysis also indicates the achievement of the encapsulation process as the presence of HA molecules in the spherical particles networks of SA. To sum up, all characterization analyses prove that HA particles were successfully encapsulated inside the SA networks in the synthesis of HAESA via aqueous sol-gel APD technique from RHA.

In vitro cell viability analysis

The cell viability assay is a primary biocompatibility test to evaluate the biological effect of SA on human body tissues (Mohd Daud et al. 2014, Naghizadeh et al. 2015). The MTT assay was used to quantify the viability of human dermal fibroblast cells and the results are presented as the percentage of untreated groups. The percentage of cell viability of HSF 1184 after 24 and 48 hours of exposure to SA, free HA and HAESA is shown in Fig. 3.

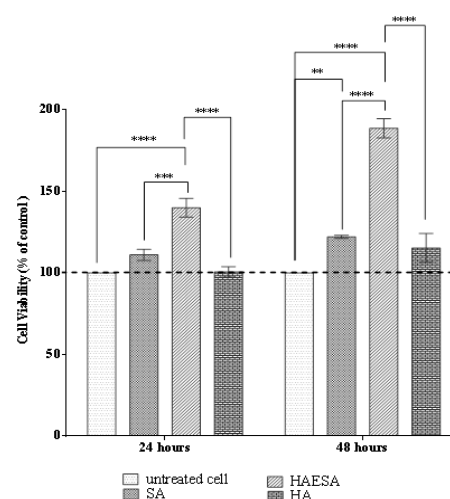


Fig. 3 Percentage of cell viability of HSF 1184 after 24 and 48 hours of exposure to SA, free HA and HAESA. The cell viability was evaluated using an MTT assay, and the results are presented as the percentage of the control groups. Data are presented as the mean \pm standard deviation (SD) of three independent experiments. * $P \leq 0.1$, ** $P \leq 0.01$, *** $P \leq 0.001$ and **** $P \leq 0.0001$ in comparison with other samples by two-way ANOVA.

The two-way ANOVA followed by Tukey post hoc test confirms that the viability of the cell growing was greater than that of the control after exposed to SA and HAESA for 24 and 48 hours (Fig. 3). These results suggest that the SA and HAESA synthesized from RHA via the aqueous sol-gel APD method was not toxic to normal human dermal fibroblasts cells and could stimulate the cells proliferation. The MTT assay also proves that HAESA could significantly stimulate cell proliferation with an increment of up to 50%, $p \leq 0.0001$, after 24 hours of exposure. Statistical analyses reveal that the fibroblastic growth was significantly ($p \leq 0.0001$) the highest when the cells were directly contacted to HAESA for both 24 and 48 hours compared to SA and HA.

In vitro cell migration analysis

The effect of HAESA (1 g/mL) on the migration of HSF 1184 cells was investigated by cells migration assay where it was conducted by exposing the cells to various extraction days (2, 5 and 7 days) of HAESA for 24 hours. The migration behaviour of the HSF 1184 cells were monitored microscopically at 0, 6, 12 and 24 hours after scratching (Fig. 4 I) and were then quantitatively determined their closure rate using ImageJ (Fig. 4 II-III).

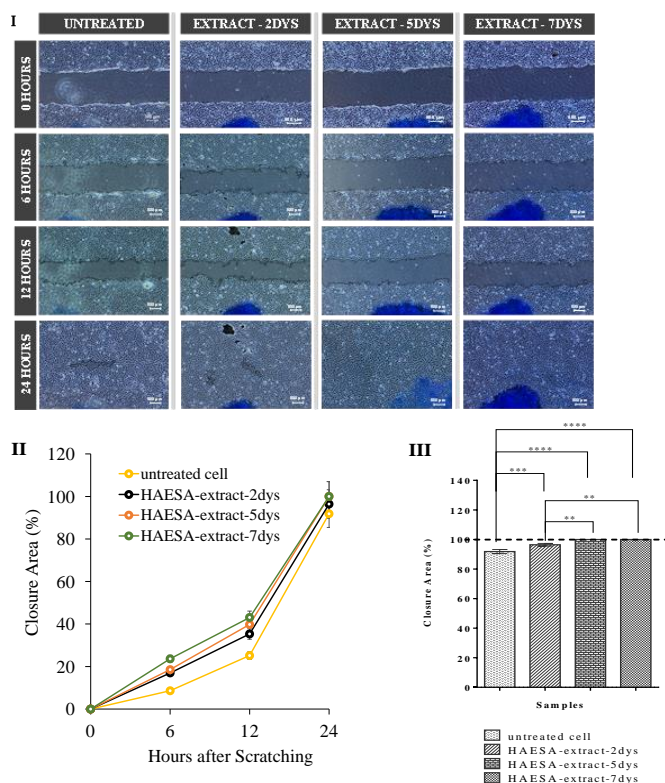


Fig. 4 (I) Images of the migration of HSF 1184 cells after (i) 0, (ii) 6, (iii) 12 and (iv) 24 hours scratching. The scratched HSF1184 cells were (a) untreated and exposed to HAESA extract, at various extraction days ((b) 2, (c) 5 and (d) 7 days). A mark that visualized at the bottom of these pictures was done to locate the same area of the scratch place. The images were obtained using an inverted optical microscope, magnification $4\times/0.13$ and scale bar of $500\ \mu\text{m}$. (II) Percentage of closure area of HSF 1184 cells after 0, 6, 12 and 24 hours scratching. (III) Percentage of closure area of HSF 1184 cells after 24 hours scratching. Data are presented as the mean \pm standard deviation (SD) of three independent experiments. $**P \leq 0.01$, $***P \leq 0.001$ and $****P \leq 0.0001$ in comparison with other samples by one-way ANOVA.

The cell migration was significantly ($p < 0.001$ - $p < 0.0001$) stimulated by HAESA after 24 hours of scratching. As depicted in Fig. 4 I, the closure area was influenced by the different extraction time, which increases with the increasing days of extraction. At 6

hours after scratching, almost 17% of the scratched area was closed after treated with HAESA-extract-2dys (sample extracted for 2 days). Further increase in the extraction time from 5 to 7 days resulted in the increase of closure area up to 24%, and the closure area was the highest when HAESA-extract-7dys was consumed by the scratched cells (Fig. 4 II). At 24 hours of scratching, all extract HAESAs significantly ($p < 0.001$ - $p < 0.0001$) enhance the cell migration (Fig. 4 III) compared to untreated cells. Both HAESA-extract-5dys and HAESA-extract-7dys, which were extracted for 5 and 7 days, respectively, led to a significantly ($p < 0.0001$) higher migration rate with 100% closure than that of the untreated control. Thus, this result indicates that silicic acid (silica) that release from HAESA, significantly play an important role in inducing and promoting human dermal fibroblast cells healing and migration.

The silicic acid concentrations (mg/L) released into the media in the presence of HSF 1184 cells and the percentage loss of silicic acid in media after 24 hours of incubation were determined in order to study the effect of physicochemical and resorbable properties of HAESA on the HSF 1184 (Fig. 5). Fig. 5 shows a graph of the percentage loss of silicic acid in media and concentration (mg/L) of silicic acid released into media after 24 hours exposed to HAESA extracts, at various extraction days (2, 5 and 7 days).

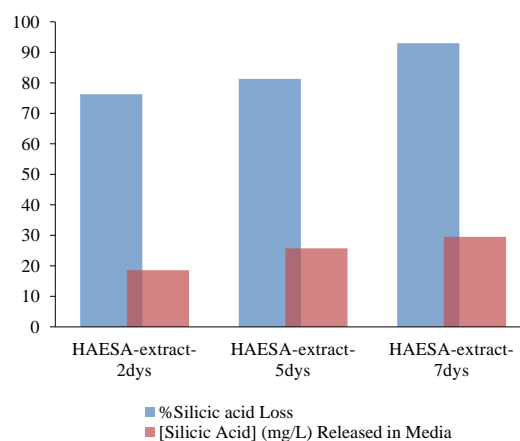


Fig. 5 Percentage loss of silicic acid in media and concentration (mg/L) of silicic acid released into media after 24 hours exposed to HAESA extracts, at various extraction days (2, 5 and 7 days).

Fig. 5 proves that silicic acid was released from the HAESAs and its concentration is increased with increase days of extraction. On 24th hours of incubation, Fig. 5 also shows that the percentage loss of silicic acid increased with the increasing extraction days of HAESA. Almost 95% of silicic acid lost in media after treated with HAESA-extract-7dys compared to HAESA-extract-2dys and HAESA-extract-5dys. This could be attributable to the uptake of silica by cells (Quignard *et al.* 2012, Kalia *et al.* 2016). Interestingly, cell migration results (Fig. 4) show the fibroblast cells that were treated with HAESAs were significantly proliferated and migrated than that of untreated. Thus, Fig. 5 proves the percentage of cells was found to depend largely on the concentration of silicic acid. The increase in fibroblast cell proliferation and migration suggest that the ionic dissolution products containing silicic acid actively stimulating a biological response in fibroblast cells and benefit fibroblast cell growth (Shie *et al.* 2011).

In this work, results have shown that the hydroxyapatite encapsulated silica aerogel (HAESA) from RHA, which was prepared via the aqueous sol-gel APD method, has no toxic potential and compatible to human dermal fibroblast cells, HSF 1184. It stimulates cells growth, spreading and enhance the cell healing and migration. Results validate that the HAESA simultaneously resorbed and the appropriate amount of released silica stimulate the fibroblastic growth and enhance migration activity of normal human fibroblasts cells.

CONCLUSION

Hydroxyapatite encapsulated silica aerogel (HAESA) was successfully synthesized from rice husk ash (RHA) via a sol-gel ambient-pressure drying (APD) method. HAESA has the ability in becoming a biocompatible and bio-inductive material to a normal human dermal fibroblast cells (HSF1184). The cell migration significantly stimulated by HAESA after 24 hours of scratching and the closure area was influenced by the different extraction time, which increases with the increasing extraction time. At 24 hours of scratching, all extract HAESA significantly enhance cell migration with 100% closure compared to the untreated control. The amount of silicic acid (silica) released from HAESA significantly play an important role in inducing and promoting human dermal fibroblast cells healing and migration. It was simultaneously resorbed in media and alteration the HA surfaces by encapsulating it inside the SA networks, consequently stimulating cell proliferation of the human dermal fibroblast cells. Thus, enabling the HAESA synthesized from RHA via the sol-gel APD technique to be used as a carrier and cell delivery vehicle, with enhanced performance such as for implant and wound care applications.

ACKNOWLEDGEMENT

Authors would like to thank to staff in Faculty of Biosciences and Medical Engineering (FBME), UTM. This project was funded by Research Grant University (RUG) (Vot 13H53) provided by UTM and Ministry of Higher Education, Malaysia.

REFERENCES

- Aminian, A., Solati-Hashjin, M., Samadikuchaksaraei, A., Bakhshi, F., Gorjipour, F., Farzadi, A., Moztarzadeh, F., and Schmücker, M., 2011. Synthesis of silicon-substituted hydroxyapatite by a hydrothermal method with two different phosphorous sources. *Ceramics International*, 37 (4), 1219–1229.
- Bohner, M., 2009. Silicon-substituted calcium phosphates - A critical view. *Biomaterials*, 30 (32), 6403–6406.
- Bohner, M., 2010. Resorbable biomaterials as bone graft substitutes. *Materials Today*, 13 (1–2), 24–30.
- Buck, D.W., Alam, M., and Kim, J.Y.S., 2009. Injectable fillers for facial rejuvenation: A review. *Journal of Plastic, Reconstructive and Aesthetic Surgery*, 62 (1), 11–18.
- Cai, H., Sharma, S., Liu, W.W., Mu, W., Liu, W.W., Zhang, X., and Deng, Y., 2014. Aerogel microspheres from natural cellulose nanofibrils and their application as cell culture scaffold. *Biomacromolecules*, 15 (7), 2540–2547.
- Dutta, S.R., Passi, D., Singh, P., and Bhuibhar, A., 2015. Ceramic and non-ceramic hydroxyapatite as a bone graft material: A brief review. *Irish Journal of Medical Science*, 184 (1), 101–106.
- Freshney, R.I., 2005. Culture of Animal Cell: A Manual of Basic Technique. *John Wiley & Sons, Inc.* John Wiley & Sons, Inc., Burbank, CA, USA.
- Fu, Q., Saiz, E., Rahaman, M.N., and Tomsia, A.P., 2011. Bioactive glass scaffolds for bone tissue engineering: State of the art and future perspectives. *Materials Science and Engineering C*, 31 (7), 1245–1256.
- Funt, D. and Pavicic, T., 2013. Dermal fillers in aesthetics: An overview of adverse events and treatment approaches. *Clinical, Cosmetic and Investigational Dermatology*, 6, 295–316.
- He, S., Huang, D., Bi, H., Li, Z., Yang, H., and Cheng, X., 2015. Synthesis and characterization of silica aerogels dried under ambient pressure bed on water glass. *Journal of Non-Crystalline Solids*, 410, 58–64.
- Hench, L.L., 1991. Bioceramics: From concept to clinic. *Journal of the American Ceramic Society*, 74 (7), 1487–1510.
- Henstock, J.R., Canham, L.T., and Anderson, S.I., 2015. Silicon: The evolution of its use in biomaterials. *Acta Biomaterialia*, 11 (1), 17–26.
- Hing, K.A., Revell, P.A., Smith, N., and Buckland, T., 2006. Effect of silicon level on rate, quality and progression of bone healing within silicate-substituted porous hydroxyapatite scaffolds. *Biomaterials*, 27 (29), 5014–5026.
- Jacovella, P.F., 2008. Use of calcium hydroxylapatite (Radiess) for facial augmentation. *Clinical interventions in aging*, 3 (1), 161–174.
- Justus, C., Leffler, N., Ruiz-Echevarria, M., and Yang, L., 2013. In vitro cell migration and invasion assays. *Mutation Research*, 752, 10–24.
- Kalia, P., Brooks, R.A., Kinrade, S.D., Morgan, D.J., Brown, A.P., Rushton, N., and Jugdaohsingh, R., 2016. Adsorption of amorphous silica nanoparticles onto hydroxyapatite surfaces differentially alters surface properties and adhesion of human osteoblast cells. *PLoS ONE*, 11 (2), 1–15.
- Kawai, K., Larson, B.J., Ishise, H., Carre, A.L., Nishimoto, S., Longaker, M., and Lorenz, H.P., 2011. Calcium-based nanoparticles accelerate skin wound healing. *PLoS ONE*, 6 (11), e27106–e27119.
- Kuhne, U. and Imhof, M., 2012. Treatment of the ageing hand with dermal fillers. *Journal of cutaneous and aesthetic surgery*, 5 (3), 163–169.
- Li, P., Ohtsuki, C., Kokubo, T., Nakanishi, K., Soga, N., and de Groot, K., 1994. The role of hydrated silica, titania, and alumina in inducing apatite on implants. *Journal of Biomedical Materials Research*, 28 (1), 7–15.
- Listiorini, E., Ramli, Z., and Hamdan, H., 1996. Optimization and reactivity study of silica in the synthesis of zeolites from rice husk. *Jurnal Teknologi*, 25, 27–35.
- Lu, T., Li, Q., Chen, W., and Yu, H., 2014. Composite aerogels based on dialdehyde nanocellulose and collagen for potential applications as wound dressing and tissue engineering scaffold. *Composites Science and Technology*, 94, 132–138.
- Mastrogiacomo, M., Muraglia, A., Komlev, V., Peyrin, F., Rustichelli, F., Crovace, A., and Cancedda, R., 2005. Tissue engineering of bone: Search for a better scaffold. *Orthodontics and Craniofacial Research*, 8 (4), 277–284.
- Mohd Daud, N., Sing, N.B., Yusop, A.H., Abdul Majid, F.A., and Hermawan, H., 2014. Degradation and in vitro cell-material interaction studies on hydroxyapatite-coated biodegradable porous iron for hard tissue scaffolds. *Journal of Orthopaedic Translation*, 2 (4), 177–184.
- Naghizadeh, F., Abdul Kadir, M.R., Doostmohammadi, A., Roozbahani, F., Iqbal, N., Taheri, M.M., Naveen, S.V., and Kamarul, T., 2015. Rice husk derived bioactive glass-ceramic as a functional bioceramic: Synthesis, characterization and biological testing. *Journal of Non-Crystalline Solids*, 427, 54–61.
- Nayak, J.P., Kumar, S., and Bera, J., 2010. Sol-gel synthesis of bioglass-ceramics using rice husk ash as a source for silica and its characterization. *Journal of Non-Crystalline Solids*, 356 (28–30), 1447–1451.
- Orlovskii, V.P., Komlev, V.S., and Barinov, S.M., 2002. Hydroxyapatite and hydroxyapatite-based ceramics. *Inorganic Materials*, 38 (10), 973–984.
- Owens, G.J., Singh, R.K., Foroutan, F., Alqaysi, M., Han, C.M., Mahapatra, C., Kim, H.W., and Knowles, J.C., 2016. Sol-gel based materials for biomedical applications. *Progress in Materials Science*, 77, 1–79.
- Perumal, S., Ramadass, S.K., and Madhan, B., 2014. Sol-gel processed mupirocin silica microspheres loaded collagen scaffold: A synergistic bio-composite for wound healing. *European Journal of Pharmaceutical Sciences*, 52 (1), 26–33.
- Porter, A.E., Patel, N., Skepper, J.N., Best, S.M., and Bonfield, W., 2003. Comparison of in vivo dissolution processes in hydroxyapatite and silicon-substituted hydroxyapatite bioceramics. *Biomaterials*, 24 (25), 4609–4620.
- Quignard, S., Mosser, G., Boissière, M., and Coradin, T., 2012. Long-term fate of silica nanoparticles interacting with human dermal fibroblasts. *Biomaterials*, 33 (17), 4431–4442.
- Rahaman, M.N., Day, D.E., Sonny Bal, B., Fu, Q., Jung, S.B., Bonewald, L.F., Tomsia, A.P., Rahamana, M.N., Daya, D.E., Balb, B.S., Fuc, Q., Junga, S.B., Bonewalde, L.F., and Tomsia, A.P., 2011. Bioactive glass in tissue engineering. *Acta Biomaterialia*, 7 (6), 2355–2373.
- Rismanchian, M., Khodaeian, N., Bahramian, L., Fathi, M., and Sadeghi-Aliabadi, H., 2013. In-vitro comparison of cytotoxicity of two bioactive glasses in micropowder and nanopowder forms. *Iranian Journal of Pharmaceutical Research*, 12 (3), 437–443.
- Rivera-Muñoz, E.M., Huirache-Acuña, R., Velázquez, R., Alonso-Núñez, G., and Eguía-Eguía, S., 2011. Growth of hydroxyapatite nanoparticles on silica gels. *Journal of Nanoscience and Nanotechnology*, 11 (6), 5592–5598.
- Rodríguez-Lorenzo, L.M. and Gross, K.A., 2003. Encapsulation of apatite particles for improvement in bone regeneration. *Journal of Materials Science: Materials in Medicine*, 14 (11), 939–943.
- Salinas, A.J. and Vallet-Regí, M., 2013. Bioactive ceramics: From bone grafts to tissue engineering. *RSC Advances*, 3 (28), 11116–11131.
- Sani, S., Mohd Muhid, M.N., and Hamdan, H., 2011. Design, synthesis and activity study of tyrosinase encapsulated silica aerogel (TESA) biosensor for phenol removal in aqueous solution. *Journal of Sol-Gel Science and Technology*, 59 (1), 7–18.

- Shie, M.Y., Ding, S.J., and Chang, H.C., 2011. The role of silicon in osteoblast-like cell proliferation and apoptosis. *Acta Biomaterialia*, 7 (6), 2604–2614.
- Srl, K.I., 2017. Kalilight: Functionalized hydroxyapatite. *kalichem*, 1–8.
- Takadama, H., Kim, H.-M., Kokubo, T., and Nakamura, T., 2001. Mechanism of biomineralization of apatite on a sodium silicate glass: TEM–EDX study in vitro. *Chemistry of Materials*, 13 (3), 1108–1113.
- Thian, E.S., Huang, J., Best, S.M., Barber, Z.H., and Bonfield, W., 2007. Silicon-substituted hydroxyapatite: The next generation of bioactive coatings. *Materials Science and Engineering C*, 27 (2), 251–256.
- Vallet-Regí, M. and Arcos, D., 2005. Silicon substituted hydroxyapatites. A method to upgrade calcium phosphate based implants. *Journal of Materials Chemistry*, 15 (15), 1509–1516.
- Wang, X., Ahmed, N. Ben, Alvarez, G.S., Tuttolomondo, M. V, Hélyary, C., Desimone, M.F., and Coradin, T., 2015. Sol-gel encapsulation of biomolecules and cells for medicinal applications. *Current topics in medicinal chemistry*, 15 (3), 223–244.
- Ylänen, H., Karlsson, K.H., Itälä, A., and Aro, H.T., 2000. Effect of immersion in SBF on porous bioactive bodies made by sintering bioactive glass microspheres. *Journal of Non-Crystalline Solids*, 275 (1), 107–115.
- Yue, P.Y.K., Leung, E.P.Y., Mak, N.K., and Wong, R.N.S., 2010. A simplified method for quantifying cell migration/wound healing in 96-well plates. *Journal of Biomolecular Screening*, 15 (4), 427–433.
- Zhang, R.Y. and Ma, P.X., 1999. Poly(alpha-hydroxyl acids) hydroxyapatite porous composites for bone-tissue engineering. I. Preparation and morphology. *Journal of Biomedical Materials Research*, 44 (4), 446–455.